


# Segmental involvement of the corpus callosum in *C9orf72*-associated ALS: a tract of interest-based DTI study

Hans-Peter Müller, Dorothée Lulé, Francesco Roselli, Anna Behler, Albert C. Ludolph and Jan Kassubek 

Ther Adv Chronic Dis

2021, Vol. 12: 1–9

DOI: 10.1177/  
20406223211002969

© The Author(s), 2021.  
Article reuse guidelines:  
sagepub.com/journals-  
permissions

## Abstract

**Background:** *C9orf72* hexanucleotide repeat expansions are associated with widespread cerebral alterations, including white matter alterations. However, there is lack of information on changes in commissure fibres. Diffusion tensor imaging (DTI) can identify amyotrophic lateral sclerosis (ALS)-associated patterns of regional brain alterations at the group level. The objective of this study was to investigate the structural connectivity of the corpus callosum (CC) in ALS patients with *C9orf72* expansions.

**Methods:** DTI-based white matter mapping was performed by a hypothesis-guided tractwise analysis of fractional anisotropy (FA) maps for 25 ALS patients with *C9orf72* expansion versus 25 matched healthy controls. Furthermore, a comparison with a patient control group of 25 sporadic ALS patients was performed. DTI-based tracts that originate from callosal sub-areas I to V were identified and correlated with clinical data.

**Results:** The analysis of white matter integrity demonstrated regional FA reductions for tracts of the callosal areas II and III for ALS patients with *C9orf72* expansions while FA reductions in sporadic ALS patients were observed only for tracts of the callosal area III; these reductions were correlated with clinical parameters.

**Conclusion:** The tract-of-interest-based analysis showed a microstructural callosal involvement pattern in *C9orf72*-associated ALS that included the motor segment III together with frontal callosal connections, as an imaging signature of the *C9orf72*-associated overlap of motor neuron disease and frontotemporal pathology.

**Keywords:** amyotrophic lateral sclerosis, *C9orf72* expansion, diffusion tensor imaging, magnetic resonance imaging, motor neuron disease

Received: 8 February 2021; revised manuscript accepted: 24 February 2021.

## Introduction

Amyotrophic lateral sclerosis (ALS) is the most frequent adult onset motor neuron disease, simultaneously affecting upper motor neurons and lower motor neurons in the brain and spinal cord; the neurodegenerative syndrome shares pathobiological features with frontotemporal dementia (FTD) so that up to 15% of patients fulfil criteria of both diseases.<sup>1</sup> In 5–10% of ALS patients, a positive family history for ALS can be detected (familial ALS, fALS),<sup>2</sup> and there is increasing evidence that the autosomal dominant

inheritance of a hexanucleotide expansion in the first intron of the *C9orf72* gene is the most common cause of fALS in people of Northern European ancestry and is also a major contributor to frontotemporal pathology in ALS.<sup>3–5</sup> The most comprehensive neuroanatomical characterization of the *C9orf72* genotype has been provided by detailed postmortem histopathology studies, but the search for *in vivo* biomarkers of disease onset and progression in *C9orf72* repeat expansion carriers has also yielded promising candidates with a focus on neuroimaging.<sup>6</sup> By

Correspondence to:

Jan Kassubek,  
Department of Neurology,  
University of Ulm, Oberer  
Eselsberg 45, Ulm, 89081,  
Germany  
jan.kassubek@uni-ulm.de

Hans-Peter Müller  
Dorothée Lulé  
Francesco Roselli  
Anna Behler  
Albert C. Ludolph

Department of Neurology,  
University of Ulm, Ulm,  
Germany



use of diffusion tensor imaging (DTI), the quantification of the diffusion properties, typically described as fractional anisotropy (FA), has been used to evaluate the neuronal fibre integrity, directional coherence and tissue microstructure in the brain. Previous data-driven DTI studies in patients with *C9orf72* expansion in cross-sectional and longitudinal design demonstrated alterations in motor tracts<sup>6–8</sup>; in addition, further white matter areas and several white matter tracts were found to be affected,<sup>9</sup> for example, in the frontal white matter.<sup>8,10</sup> A recent study demonstrated *in vivo* histopathological staging specifically in *C9orf72*-associated ALS by application of a tract of interest (TOI)-based DTI analysis technique.<sup>8,11,12</sup>

Corpus callosum (CC) degeneration is a recognised feature of ALS and has been consistently highlighted by post mortem studies and demonstrated repeatedly *in vivo* by computational neuroimaging as part of the widespread white matter changes in ALS.<sup>13–19</sup> A recent study demonstrated *in vivo* histopathological staging specifically in *C9orf72*-associated ALS by application of a TOI-based DTI analysis technique.<sup>8,11,12</sup> It has been demonstrated that genotype-specific changes in *C9orf72* associated ALS can be observed in commissure fibres including the anterior CC.<sup>20</sup> Pathology of callosal damage in ALS by an *ex vivo* 7T MRI study showed increased microglial cells in the body of the CC, especially in cases with *C9orf72* mutations, and increased reactive astrocytes throughout the CC.<sup>21</sup> Obviously, the fibre changes were not distributed equally along the callosal structure but had a distinct pattern along the CC in ALS.<sup>22</sup> According to fibre tractography studies,<sup>23</sup> the CC can be subdivided into five different structural areas: I–V. How ALS-associated fibre changes of the CC follow these structural areas and whether the CC affection pattern is distinctly different between genotypes is unclear. Of special interest are those patients carrying *C9orf72* mutations as these are expected to be associated with the most severe microstructural alterations and thus the most widespread white matter alterations.<sup>24</sup>

In the current study, the TOI-based analysis of DTI data was applied to the five different CC areas according to Hofer and Frahm in ALS patients with *C9orf72* expansion, in order to investigate *in vivo* the specific callosal alteration pattern.<sup>23</sup>

## Materials and methods

### *Subjects and patient characteristics*

A total of 25 ALS patients with confirmed *C9orf72* expansion mutations were included. Clinically they met the revised El Escorial diagnostic criteria.<sup>25</sup> Four of the *C9orf72* expansion carriers fulfilled the criteria for ALS-FTD of the behavioural type (bvFTD) according to Rascovsky criteria.<sup>2</sup> Details of demographics, clinical data including the revised ALS functional rating scale (ALS-FRS-R),<sup>26</sup> slope of ALS-FRS-R as an indicator for disease progression, upper motor neuron (UMN) burden score,<sup>27</sup> site of onset, and disease duration are summarized in Table 1.

ALS patients with *C9orf72* expansions were compared first, with a group of 25 age- and gender-matched controls and second, with a group of 25 sporadic ALS patients who had no family history of motor neuron disease (MND) and had been tested negative for the major genes related to ALS (Table 1). Gross brain pathology, including vascular brain alterations, could be excluded by conventional MRI including fluid attenuated inversion recovery sequences. All control individuals lacked a family history of neuromuscular disease and had no history of neurological, psychiatric or other major medical illnesses and were recruited from among spouses of patients and by word of mouth.

All participants provided written informed consent for the study protocol according to institutional guidelines which had been approved by the Ethics Committee of Ulm University, Germany (No. 19/12).

### *Genetic analysis*

DNA was extracted from whole EDTA-containing venous blood samples as previously described. Analysis of the *C9orf72* repeat length was performed by fragment length analysis and repeat-primed PCR (RP-PCR) using previously published primers.<sup>29</sup> Since PCR-based methods cannot determine the size of larger expanded repeat-alleles, samples with a sawtooth pattern in the RP-PCR were further analysed using Southern blot.<sup>3</sup>

### *Magnetic resonance imaging acquisition*

Magnetic resonance imaging (MRI) scans were obtained on a 1.5 Tesla Magnetom Symphony scanner (Siemens Medical, Erlangen, Germany).

**Table 1.** Subject characteristics including disease duration, site of onset, ALS-FRS-R, disease progression rate (slope of ALS-FRS-R), UMN burden score,<sup>27</sup> and cognitive profile measured by the ECAS.<sup>28</sup>

	Gender (m/f)	Age (years)	Disease duration (months median)	Site of onset bulbar/spinal	ALS-FRS-R median	ALS-FRS-R slope median	UMN burden score	ECAS total score
<i>C9orf72</i> -associated ALS	17/8	63 ± 11 (range 35–79)	12, range 3–37	10/15	41 (range 27–48)	–13/year range [–1 to –31]/year	7 ± 6 range [2–14]	30 ± 8
Sporadic ALS	14/11	64 ± 11 (range 31–83)	11, range 5–28	7/18	43 (range 30–48)	–8/year range [–1 to –28]/year	7 ± 4 range [2–14]	Not available
Controls	18/7	63 ± 16 (range 26–80)	–	–	–	–	–	–
<i>p</i>	Kruskal–Wallis 0.62	Kruskal–Wallis 0.81	<i>t</i> test 0.98	–	<i>t</i> test 0.80	<i>t</i> test 0.64	<i>t</i> test 0.16	

ALS, amyotrophic lateral sclerosis ; ALS-FRS-R, revised ALS functional rating scale; ECAS, Edinburgh cognitive and behavioral ALS screen; f, female; m, male; UMN, upper motor neuron.

**Table 2.** Association analysis of TFAS-based FA values of tracts of CC areas I–V with the clinical parameters (disease duration, ALS-FRS-R and UMN burden score).

	Clinical parameter	CC area I tracts	CC area II tracts	CC area III tracts	CC area IV tracts	CC area V tracts
<i>C9orf72</i> -associated ALS	Disease duration	–0.21	–0.09	–0.51*	–0.14	–0.11
	ALS-FRS-R	–0.04	0.12	0.40*	–0.19	–0.02
	UMN burden score	–0.02	–0.43*	–0.61*	0.00	–0.10
Sporadic ALS	Disease duration	0.25	0.09	–0.01	0.07	0.27
	ALS-FRS-R	0.23	0.39	0.43*	0.20	0.14
	UMN burden score	–0.36	–0.56*	–0.52*	–0.38	–0.31

\*Significant correlation.  
ALS, amyotrophic lateral sclerosis ; ALS-FRS-R, revised ALS functional rating scale; CC, corpus callosum; FA, fractional anisotropy; TFAS, tractwise fractional anisotropy statistics; UMN, upper motor neuron.

The DTI study protocol consisted of 52 volumes (64 slices, 128 × 128 pixels, slice thickness 2.8 mm, pixel size 2.0 mm × 2.0 mm), representing 48 gradient directions ( $b = 1000 \text{ s/mm}^2$ ) and four scans with  $b = 0$ ; TE and TR were 95 ms and 8000 ms, respectively.

#### Data analysis

DTI data were analysed with the software Tensor Imaging and Fibre Tracking (TIFT).<sup>30</sup> The

algorithms used in this study have been described previously in detail.<sup>11,12,31</sup> In short, stereotaxic normalization to the Montreal Neurological Institute (MNI) space was performed iteratively by combined linear and non-linear registration using study-specific templates.<sup>32</sup> From the stereotaxically normalized DTI data sets of all subjects, individual FA maps were calculated quantitatively. A Gaussian filter of 8 mm full width at half maximum was applied for smoothing of the individual FA maps in order to reduce

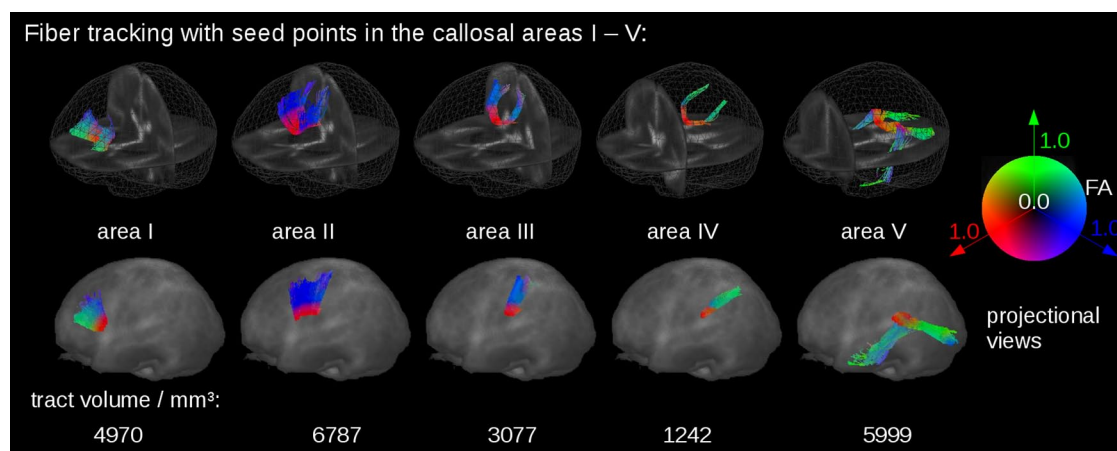


**Figure 1.** Tracts of the different segments of the CC with starting seeds for fibre tracking in callosal areas I–V of the median sagittal slice. The fibre tracts were calculated from the averaged data set from 25 controls. Tract volumes are given in  $\text{mm}^3$ , calculated from the number of contributing voxels. CC, corpus callosum.

residual individual morphological differences after stereotaxic normalization.<sup>33</sup> Finally, data were corrected for the covariate age. Examples for stereotaxic CC matching are presented in Supplemental Figure S1.

From the MNI normalized data of 25 controls, an averaged data set was calculated; this data set was used for fibre tracking. That way, common FT masks could be applied to the individual FA maps. To this end, a conventional streamline tracking was used with a vector product threshold of 0.9 and an FA threshold of 0.2.<sup>34,35</sup> Subsequently, the CC could be subdivided into five areas<sup>23</sup>: area I tracts are callosal fibres comprising bundles projecting into the prefrontal lobe, area II tracts are callosal fibres projecting to frontal areas including premotor and supplementary motor cortices, area III fibres project to the primary motor cortices, area IV fibres project to primary sensory cortices, and area V fibres project to parietal lobe, occipital lobe and temporal lobe. Defined tracts originating in CC areas I–V according to this scheme were identified with the TOI approach.<sup>17</sup> Figure 1 shows the separate tracts, calculated from the averaged template (MNI normalized data of 25 controls), with starting seeds for fibre tracking depicted in the median sagittal slice (Supplemental Figure S1). The seed areas were set according to the Hofer and Frahm scheme with respect to an FA threshold of 0.2.<sup>23</sup> This seed placement has been performed in callosal areas I–V with FT seed points restricted to the CC (Supplemental Figure S1). Supplemental Figure S2 shows fibre

tracking-based end points of tracts originating in the callosal areas I–V. Tract-wise fractional anisotropy statistics (TFAS) were performed by statistically comparing the FA values in each tract between the two groups (Student's *t* test),<sup>34,36</sup> not considering FA-values below 0.2, since cortical grey matter shows FA values up to 0.2.<sup>35</sup>

A correlation analysis between individual tract-based FA-values and clinical and cognitive scores was performed with Pearson correlation. A threshold of  $p < 0.05$  (two-tailed) was used for statistical interference.

## Results

### *Structural changes in C9orf72 fALS patients*

The analysis of the regional FA differences in the CC-associated tracts by use of TFAS showed significant differences in the averaged FA values between the *C9orf72* fALS patients and the controls, as demonstrated in Figure 2. The differences were significant in the tracts of callosal areas II and III, while no significant alterations were detected in the tracts of callosal areas I, IV and V (Bonferroni-corrected for multiple comparisons). TFAS demonstrated significant differences in the averaged FA values between the sporadic ALS patients and the controls in the tracts of callosal area III, but not in the tracts of callosal area II (Figure 2). No significant alterations between *C9orf72* fALS patients and sporadic ALS patients could be detected. Results for mean

## Tractwise fractional anisotropy statistics (TFAS):

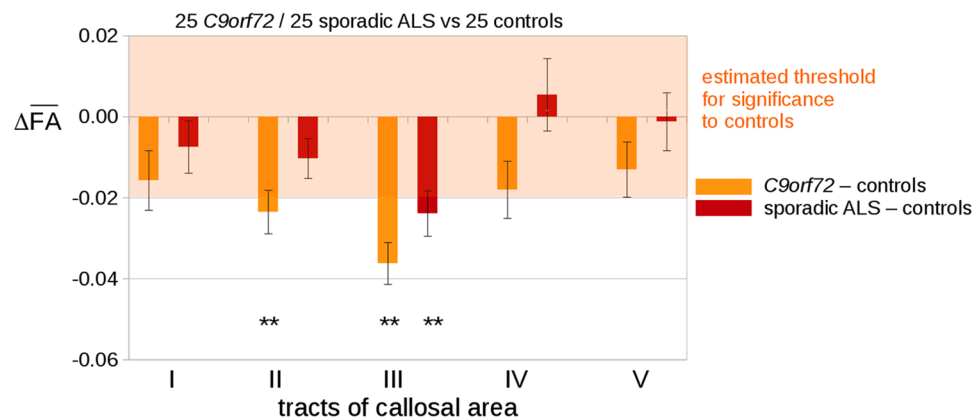


**Figure 2.** TFAS at the group level for *C9orf72* fALS patients compared with controls. TFAS demonstrated significant regional FA reductions in tracts of callosal areas II and III in *C9orf72* fALS patients compared with matched controls and FA reductions in tracts of callosal area III in sporadic ALS patients. Error bars are SEM. \* $p < 0.05$ , \*\* $p < 0.001$  (Bonferroni-corrected).

ALS, amyotrophic lateral sclerosis; FA, fractional anisotropy; fALS, familial ALS; SEM, standard error of the mean; TFAS, tractwise fractional anisotropy statistics.

FA values and corresponding  $p$  values are summarized in Supplemental Table S1.

For the *C9orf72* group, significant associations with ALS-FRS-R, UMN burden score and disease duration, respectively, were observed for the tracts of callosal area III, while no significant correlations resulted from the analysis of the tracts of the remaining callosal areas including area II. For the sporadic ALS group, significant associations with ALS-FRS-R and UMN burden score were also observed solely for the tracts of callosal area III. The results are summarized in Table 2. No associations were observed for site of onset and disease progression rate.

#### Level analysis of callosal tracts originating in areas II and III

To provide a more comprehensive profile of the callosal tracts for CC areas II and III it was investigated whether there is higher abnormality at an extra-callosal level or at the level of the CC; to this end, regions were specified along the callosal tracts, separating into CC and extra-CC (Supplemental Figure S3, Supplemental Table S2). TFAS showed significant differences for the *C9orf72* patients, related mostly to extra-callosal parts, both for tracts of areas II and III. For the sporadic ALS patients, significant differences from controls could be shown for callosal tracts of area III.

#### Association of structural and cognitive changes

FA values for the tracts of callosal areas I–V were correlated to the executive function score of the Edinburgh cognitive and behavioral ALS screen (ECAS).<sup>28</sup> For the *C9orf72* patients, a positive association was observed for tracts of callosal areas I ( $p = 0.02$ ,  $R^2 = 0.55$ ) and II ( $p = 0.06$ ,  $R^2 = 0.46$ ) to executive function, whereas tracts of callosal areas III, IV and V showed no association.

#### Discussion

The search for biomarkers in ALS with *C9orf72* repeat expansion has yielded promising candidates in the neuroimaging domain, including thalamic atrophy, global loss of functional connectivity, global volume loss (ventricular atrophy, subcortical atrophy), diffuse cortical thinning and loss of white matter integrity.<sup>9,37,38</sup> Recently, a hypothesis-driven DTI study showed a sequential corticoefferent spreading pattern in ALS with *C9orf72* expansions according to the principles of the proposed neuropathological staging concept of ALS, which is based on cerebral TDP43 pathology.<sup>8</sup> Given that data-driven DTI studies had demonstrated reduced integrity of frontal white matter and association tracts,<sup>6</sup> the current study addressed the unresolved question of whether, and to what extent, there is a DTI-based association fibre in the CC signature of *C9orf72* repeat expansion.

To this end, a hypothesis-guided TOI-based approach was applied to MRI data of patients with *C9orf72* repeat expansion-associated ALS. This technique specifically addressed the callosal white matter fibres that fan out into the white matter of both hemispheres, that is, the radiation of the CC; here, the homotopic commissural connections that interconnect the frontal lobes pass in the anterior half of the CC, while the others pass in the posterior half.<sup>39</sup> In order to reflect the DTI approach, the topological classification was performed following the scheme of Hofer and Frahm,<sup>23</sup> which was also derived from a DTI-based tract-tracing algorithm.

The results demonstrated, both for the *C9orf72* group and the sporadic ALS group that was included as a control sample, a predominant involvement of tracts of callosal area III, which also showed significant correlations with the clinical presentation (ALS-FRS-R, UMN burden score and disease duration, respectively), that is, involvement of the motor cortex; note that, in contrast to patients with sporadic ALS, tracts of callosal area II showed significant FA reductions only in *C9orf72* patients. This finding indicates a more marked frontal involvement in familial *C9orf72* patients than in sporadic ALS patients. Area II contains fibres projecting to frontal regions (including premotor and supplementary motor cortical areas), while area III comprises fibres projecting into the primary motor cortices. It has already been reported for sporadic ALS that the involvement of the CC is a consistent feature in MRI.<sup>22,40,41</sup> More specifically, CC area III, that is, the motor segment,<sup>23</sup> has been reported to demonstrate high T2 signal and regional atrophy at individual levels in routine structural MRI in MND,<sup>42</sup> and has been discussed as an imaging marker in ALS.<sup>14,15</sup> The current data are in agreement with previous studies,<sup>15,43</sup> which showed associations of the callosal motor area with UMN burden score. In a recent T1w MRI-based texture analysis, the subtype (sporadic) primary lateral sclerosis (PLS) was associated with focused regional CC atrophy and texture alterations limited to the motor-related callosal area III.<sup>44</sup> The tracts of the callosal area III showed significant FA reductions in *C9orf72* patients as well as in sporadic ALS patients. In the light of the cortico-efferent spread of pathology from the motor cortices in ALS, a separate analysis of the superior cortex-adjacent and the CC-adjacent parts of the tracts demonstrated more marked involvement

(lower FA) of the former than the latter areas, indicating indirect support of the corticoefferent model both for *C9orf72* patients and sporadic ALS patients. These findings are generally in agreement with previous DTI studies in ALS,<sup>45</sup> but remain to be confirmed in a future study with higher subject numbers.

The current DTI study thus supports the segmental involvement of tracts originating from the CC in *C9orf72* fALS. The anatomical involvement of the cerebral structures in *C9orf72* repeat expansion-associated ALS corresponds to the TDP43 propagation pattern, as reported in the original description.<sup>46</sup> Accordingly, it can be mapped by the TOI-based approach *in vivo*.<sup>8</sup> The specific involvement of the fibres interconnecting the motor cortices is another element of the fingerprint of cerebral white matter alterations in fALS patients with *C9orf72* expansion. These data are in accordance with the results of previous data-driven DTI studies,<sup>6</sup> which showed a widespread reduction of white matter integrity in this patient subgroup. The involvement of area II – which could not be demonstrated in the sporadic ALS group – is of specific interest, indicating that fronto-temporal involvement as a part of the spectrum of *C9orf72*-associated disorders might be reflected by a reduction in FA in tracts originating from more frontal CC parts, which represent fibres homotopically interconnecting the bilateral frontal cortices.

These findings await confirmation in larger groups of *C9orf72*-positive patients with clinical presentation of frontal deficits. The concept is further supported by the association of executive dysfunction and changes in frontal callosal areas I and II. Executive dysfunction is the most prominent cognitive change in behavioral variant FTD patients and ALS,<sup>47,48</sup> and executive functions are processed in dorsal frontal hemispheres that are interconnected by frontal callosal areas I and II. White matter alterations in fibres of dorsal frontal areas have been shown to be altered in association to executive dysfunction.<sup>49</sup> We hereby present evidence that changes in frontal fibres can also be shown on the callosal level. Accordingly, it can be assumed that the pattern of FA changes in frontal parts of the CC in the four FTD patients resembles a correlate of executive dysfunction also in motor type ALS patients. It also underlines previous findings of white matter alterations in frontal areas that are seen in patients with executive dysfunction at early pathological stages of ALS.<sup>50</sup>

This study was not without limitations. There was no neuropathological confirmation of the neuroimaging results by autopsy. Future studies should include longitudinal data to investigate the possibility of tracking disease propagation, as previously demonstrated for staging schemes of sporadic ALS patients.<sup>17,50,51</sup>

In summary, the results of this study in *C9orf72*-fALS demonstrate a segmental CC involvement with predominance of callosal tracts II and III where the correlation to the clinical presentation (ALS-FRS-R, UMN burden score and disease duration) is dominated by callosal tract III alterations, that is, involvement of the motor cortex. This specific characterisation of commissural white matter tracts adds novel insights to an established facet of ALS pathology.<sup>19</sup> From the clinical perspective, the involvement of the CC, and especially the callosal tracts of area II, might be utilized as a promising candidate imaging marker for cerebral white matter abnormalities in *C9orf72* fALS patients,<sup>9</sup> which also addresses the *C9orf72*-associated overlap of motor neuron disease and frontotemporal pathology. These findings may be of clinical relevance for future clinical trials, for example, persons known to carry the *C9orf72* expansion could receive DTI-based analyses at a presymptomatic stage to determine the time point in the disease course when the *in vivo* detection of the segmental CC alterations is possible.

### Acknowledgements

Sonja Fuchs is gratefully acknowledged for her help in the acquisition of MRI data. Kornelia Günther is gratefully acknowledged for her help in assembling the clinical data. The authors would like to thank the Ulm University Centre for Translational Imaging MoMAN for its support.

### Author contributions

Hans-Peter Müller: Study concept and design, data analysis and interpretation of data, critical revision of manuscript for intellectual content.

Dorothee Lulé: Neuropsychology data analysis and interpretation of data, critical revision of manuscript for intellectual content.

Francesco Roselli: Interpretation of data, critical revision of manuscript for intellectual content.

Anna Behler: Interpretation of data, critical revision of manuscript for intellectual content.

Albert C. Ludolph: Interpretation of data, critical revision of manuscript for intellectual content.

Jan Kassubek: Study concept and design, interpretation of data, study supervision, drafting of manuscript.

### Conflict of interest statement

The Associate Editor of *Therapeutic Advances in Chronic Disease* is an author of this paper, therefore, the peer review process was managed by alternative members of the Board and the submitting Editor had no involvement in the decision-making process. The authors declare that there is no conflict of interest.

### Ethical approval

All human studies have been approved by the appropriate ethics committee and have therefore been performed in accordance with the ethical standards laid down in the 1964 Declaration of Helsinki and its later amendments.

### Funding

The authors disclosed receipt of the following financial support for the research, authorship, and/or publication of this article: This study was supported by the German Research Foundation (Deutsche Forschungsgemeinschaft, DFG Grant Number LU 336/15-1), the German Network for Motor Neuron Diseases (BMBF 01GM1103A) and Deutsches Zentrum für Neurodegenerative Erkrankungen (DZNE).

### ORCID iD

Jan Kassubek  <https://orcid.org/0000-0002-7106-9270>

### Supplemental material

Supplemental material for this article is available online.

### References

1. van Es MA, Hardiman O, Chio A, *et al.* Amyotrophic lateral sclerosis. *Lancet* 2017; 390: 2084–2098.
2. Chiò A, Calvo A, Moglia C, *et al.* Phenotypic heterogeneity of amyotrophic lateral sclerosis: a population based study. *J Neurol Neurosurg Psychiatry* 2011; 82: 740–746.
3. DeJesus-Hernandez M, Mackenzie IR, Boeve BF, *et al.* Expanded GGGGCC hexanucleotide repeat in noncoding region of *C9orf72* causes chromosome 9p-linked FTD and ALS. *Neuron* 2011; 72: 245–256.

4. Renton AE, Majounie E, Waite A, *et al.* A hexanucleotide repeat expansion in C9ORF72 is the cause of chromosome 9p21-linked ALS-FTD. *Neuron* 2011; 72: 257–268.
5. Renton AE, Chiò A and Traynor BJ. State of play in amyotrophic lateral sclerosis genetics. *Nat Neurosci* 2014; 17: 17–23.
6. Floeter MK, Danielian LE, Braun LE, *et al.* Longitudinal diffusion imaging across the C9orf72 clinical spectrum. *J Neurol Neurosurg Psychiatry* 2018; 89: 53–60.
7. Agosta F, Ferraro PM, Riva N, *et al.* Structural and functional brain signatures of C9orf72 in motor neuron disease. *Neurobiol Aging* 2017; 57: 206–219.
8. Müller HP, Del Tredici K, Lulé D, *et al.* In vivo histopathological staging in C9orf72-associated ALS: a tract of interest DTI study. *Neuroimage Clin* 2020; 27: 102298.
9. Floeter MK and Gendron TF. Biomarkers for amyotrophic lateral sclerosis and frontotemporal dementia associated with hexanucleotide expansion mutations in C9orf72. *Front Neurol* 2018; 9: 1063.
10. Westeneng HJ, Walhout R, Straathof M, *et al.* Widespread structural brain involvement in ALS is not limited to the C9orf72 repeat expansion. *J Neurol Neurosurg Psychiatry* 2016; 87: 1354–1360.
11. Kassubek J and Müller HP. Advanced neuroimaging approaches in amyotrophic lateral sclerosis: refining the clinical diagnosis. *Expert Rev Neurother* 2020; 20: 237–249.
12. Kassubek J, Müller HP, Del Tredici K, *et al.* Diffusion tensor imaging analysis of sequential spreading of disease in amyotrophic lateral sclerosis confirms patterns of TDP-43 pathology. *Brain* 2014; 137: 1733–1740.
13. Agosta F, Pagani E, Petrolini M, *et al.* Assessment of white matter tract damage in patients with amyotrophic lateral sclerosis: a diffusion tensor MR imaging tractography study. *AJNR Am J Neuroradiol* 2010; 31: 1457–1461.
14. Kassubek J, Ludolph AC and Müller HP. Neuroimaging of motor neuron diseases. *Ther Adv Neurol Disord* 2012; 5: 119–127.
15. Agosta F, Galantucci S, Riva N, *et al.* Intrahemispheric and interhemispheric structural network abnormalities in PLS and ALS. *Hum Brain Mapp* 2014; 35: 1710–1722.
16. Müller HP, Turner MR, Grosskreutz J, *et al.* A large-scale multicentre cerebral diffusion tensor imaging study in amyotrophic lateral sclerosis. *J Neurol Neurosurg Psychiatry* 2016; 87: 570–579.
17. Kassubek J, Müller HP, Del Tredici K, *et al.* Imaging the pathoanatomy of amyotrophic lateral sclerosis in vivo: targeting a propagation-based biological marker. *J Neurol Neurosurg Psychiatry* 2018; 89: 374–381.
18. Tu S, Wang C, Menke RAL, *et al.* Regional callosal integrity and bilaterality of limb weakness in amyotrophic lateral sclerosis. *Amyotroph Lateral Scler Frontotemporal Degener* 2020; 21: 396–402.
19. Bede P, Siah WF, McKenna MC, *et al.* Consideration of C9orf72-associated ALS-FTD as a neurodevelopmental disorder: insights from neuroimaging. *J Neurol Neurosurg Psychiatry* 2020; 91: 1138.
20. Mahoney CJ, Beck J, Rohrer JD, *et al.* Frontotemporal dementia with the C9ORF72 hexanucleotide repeat expansion: clinical, neuroanatomical and neuropathological features. *Brain* 2012; 135: 736–750.
21. Cardenas AM, Sarlls JE, Kwan JY, *et al.* Pathology of callosal damage in ALS: an *ex-vivo*, 7 T diffusion tensor MRI study. *Neuroimage Clin* 2017; 15: 200–208.
22. Chapman MC, Jelsone-Swain L, Johnson TD, *et al.* Diffusion tensor MRI of the corpus callosum in amyotrophic lateral sclerosis. *J Magn Reson Imaging* 2014; 39: 641–647.
23. Hofer S and Frahm J. Topography of the human corpus callosum revisited—comprehensive fiber tractography using diffusion tensor magnetic resonance imaging. *Neuroimage* 2006; 32: 989–994.
24. Floeter MK, Bageac D, Danielian LE, *et al.* Longitudinal imaging in C9orf72 mutation carriers: relationship to phenotype. *Neuroimage Clin* 2016; 12: 1035–1043.
25. Ludolph A, Drory V, Hardiman O, *et al.* A revision of the El Escorial criteria - 2015. *Amyotroph Lateral Scler Frontotemporal Degener* 2015; 29: 1–2.
26. Cedarbaum JM, Stambler N, Malta E, *et al.* The ALSFRS-R: a revised ALS functional rating scale that incorporates assessments of respiratory function. BDNF ALS study group (phase III). *J Neurol Sci* 1999; 169: 13–21.
27. Turner MR, Cagnin A, Turkheimer FE, *et al.* Evidence of widespread cerebral microglial activation in amyotrophic lateral sclerosis: an [11C](R)-PK11195 positron emission



- tomography study. *Neurobiol Dis* 2004; 15: 601–609.
28. Lulé D, Burkhardt C, Abdulla S *et al.* The Edinburgh cognitive and behavioural amyotrophic lateral sclerosis screen: a cross-sectional comparison of established screening tools in a German-Swiss population. *Amyotroph Lateral Scler Frontotemporal Degener* 2015; 16: 16–23.
  29. Zondler L, Müller K, Khalaji S, *et al.* Peripheral monocytes are functionally altered and invade the CNS in ALS patients. *Acta Neuropathol* 2016; 132: 391–411.
  30. Müller HP, Unrath A, Ludolph AC, *et al.* Preservation of diffusion tensor properties during spatial normalisation by use of tensor imaging and fibre tracking on a normal brain database. *Phys Med Biol* 2007; 52: N99–N109.
  31. Müller HP and Kassubek J. MRI-based mapping of cerebral propagation in amyotrophic lateral sclerosis. *Front Neurosci* 2018; 12: 655.
  32. Müller HP, Unrath A, Riecker A, *et al.* Intersubject variability in the analysis of diffusion tensor images at the group level: fractional anisotropy mapping and fiber tracking techniques. *Magn Reson Imaging* 2009; 27: 324–334.
  33. Unrath A, Müller HP, Riecker A, *et al.* Whole brain-based analysis of regional white matter tract alterations in rare motor neuron diseases by diffusion tensor imaging. *Hum Brain Mapp* 2010; 31: 1727–1740.
  34. Müller HP, Unrath A, Sperfeld AD, *et al.* Diffusion tensor imaging and tractwise fractional anisotropy statistics: quantitative analysis in white matter pathology. *Biomed Eng Online* 2007; 6: 42.
  35. Kunimatsu A, Aoki S, Masutani Y, *et al.* The optimal trackability threshold of fractional anisotropy for diffusion tensor tractography of the corticospinal tract. *Magn Reson Med Sci* 2004; 3: 11–17.
  36. Müller HP, Grön G, Sprengelmeyer R, *et al.* Evaluating multicenter DTI data in Huntington's disease on site specific effects: an ex post facto approach. *Neuroimage Clin* 2013; 2: 161–167.
  37. Floeter MK, Traynor BJ, Farren J, *et al.* Disease progression in *C9orf72* mutation carriers. *Neurology* 2017; 89: 234–241.
  38. Chipika RH, Siah WF, McKenna MC, *et al.* The presymptomatic phase of amyotrophic lateral sclerosis: are we merely scratching the surface? *J Neurol*. Epub ahead of print 31 October 2020. DOI: 10.1007/s00415-020-10289-5.
  39. Nieuwenhuys R, Voogd J and van Huijzen C. *The Human Central Nervous System*. Heidelberg: Steinkopff-Verlag, 2019.
  40. Filippini N, Douaud G, Mackay CE, *et al.* Corpus callosum involvement is a consistent feature of amyotrophic lateral sclerosis. *Neurology* 2010; 75: 1645–1652.
  41. Müller HP, Unrath A, Huppertz HJ, *et al.* Neuroanatomical patterns of cerebral white matter involvement in different motor neuron diseases as studied by diffusion tensor imaging analysis. *Amyotroph Lateral Scler* 2012; 13: 254–264.
  42. Osborn AG, Hedlund GL and Salzman KL. *Osborn's brain*. Philadelphia, PA: Elsevier - Health Sciences Division, 2017.
  43. Cirillo M, Esposito F, Tedeschi G, *et al.* Widespread microstructural white matter involvement in amyotrophic lateral sclerosis: a whole-brain DTI study. *AJNR Am J Neuroradiol* 2012; 33: 1102–1108.
  44. Müller HP, Dreyhaupt J, Roselli F, *et al.* Focal alterations of the callosal area III in primary lateral sclerosis: an MRI planimetry and texture analysis. *Neuroimage Clin* 2020; 26: 102223.
  45. Gabel MC, Broad RJ, Young AL, *et al.* Evolution of white matter damage in amyotrophic lateral sclerosis. *Ann Clin Transl Neurol* 2020; 7: 722–732.
  46. Brettschneider J, Del Tredici K, Toledo JB, *et al.* Stages of pTDP-43 pathology in amyotrophic lateral sclerosis. *Ann Neurol* 2013; 74: 20–38.
  47. Rascovsky K, Hodges JR, Knopman D, *et al.* Sensitivity of revised diagnostic criteria for the behavioural variant of frontotemporal dementia. *Brain* 2011; 134: 2456–2477.
  48. Phukan J, Elamin M, Bede P, *et al.* The syndrome of cognitive impairment in amyotrophic lateral sclerosis: a population-based study. *J Neurol Neurosurg Psychiatry* 2012; 83: 102–108.
  49. Pettit LD, Bastin ME, Smith C, *et al.* Executive deficits, not processing speed relates to abnormalities in distinct prefrontal tracts in amyotrophic lateral sclerosis. *Brain* 2013; 136: 3290–3304.
  50. Lulé D, Böhm S, Müller HP, *et al.* Cognitive phenotypes of sequential staging in amyotrophic lateral sclerosis. *Cortex* 2018; 101: 163–171.
  51. Kalra S, Müller H-P, Ishaque A, *et al.* A prospective harmonized multicentre DTI study of cerebral white matter degeneration in ALS. *Neurology* 2020; 95: e943–e952.